Radiotherapy and Oncology 141 (2019) 262–266

Contents lists available at ScienceDirect

Radiotherapy and Oncology

journal homepage: www.thegreenjournal.com

Short Communication

DNA damage enhancement by radiotherapy-activated hafnium oxide nanoparticles improves cGAS-STING pathway activation in human colorectal cancer cells

Julie Marill, Naeemunnisa Mohamed Anesary, Sébastien Paris *

Nanobiotix, Paris, France

ARTICLE INFO

Article history:
Received 29 May 2019
Received in revised form 8 July 2019
Accepted 20 July 2019
Available online 19 August 2019

Keywords:
Nanoparticle
NBTXR3
cGAS-STING
Colorectal cancer
Radiotherapy

ABSTRACT

The cGAS-STING pathway can be activated by radiation induced DNA damage and because of its important role in anti-cancer immunity activation, methods to increase its activation in cancer cells could provide significant therapeutic benefits for patients. We explored the impact of hafnium oxide nanoparticles (NBTXR3) activated by radiotherapy on cell death, DNA damage, and activation of the cGAS-STING pathway. We demonstrate that NBTXR3 activated by radiotherapy enhances cell destruction, DNA double strand breaks, micronuclei formation and cGAS-STING pathway activation in a human colorectal cancer model, compared to radiotherapy alone.

Currently, around 60% of all cancer patients receive RT as part of their treatment [1]. While the main antitumor effect of radiotherapy (RT) is induction of DNA double strand breaks (DSBs) [2], preclinical and clinical studies show that RT can also modulate both the innate and adaptive immune system [3,4]. For instance, RT can induce the immunogenic cell death [4,5], increase MHC-I expression on cancer cells [6]. In addition, DNA damage induced by the RT can trigger formation of free DNA in the cytoplasm. The DNA sensor cGAS will bind this free DNA, triggering the production of cGAMP, which will activate STING. Activated-STING will allow IRF3/7 transcription factor to enter into the nucleus, leading to type-I interferon (IFN-1) secretion [7]. IFN-1 production in the tumor microenvironment is required to recruit Batf3-dependent dendritic cells (DC) to poorly immunogenic tumors, subsequent T-cell activation, and tumor cell killing. In addition, activation of the cGAS-STING pathway has also been shown to be essential for the activity of immune checkpoint inhibitors (ICIs) [8]. Thus, activation of the cGAS-STING pathway has become an attractive therapeutic target with the potential to prime anti-cancer immune response and to improve the efficacy of ICIs [4,9–11].

The high electron density of functionalized hafnium oxide nanoparticles (NBTXR3) allows a high probability of interaction with incoming ionizing radiation (when compared to cancer cells mostly constituted of low electron density molecules, like water) and an increased energy dose deposit within cancer cells. Due to this physical mode of action, we have previously reported that treatment with NBTXR3 activated by RT yielded increased cancer cell death and better local tumor growth control than RT alone [12–14]. NBTXR3 is currently being evaluated in several clinical trials and positive topline results were recently reported for a phase II/III trial in patients with locally advanced soft tissue sarcoma [15].

Here, we examined the effect of NBTXR3 activated by RT on cell death, DNA damage, and activation of the cGAS-STING pathway in the human colorectal cancer HCT116-DUAL cells. We show that RT-activated NBTXR3 significantly increases cell killing, DSBs and micronuclei formation, compared to RT alone. We also demonstrate that the cGAS-STING pathway was starkly more active in cells treated by NBTXR3 and RT, than that observed in cells that only received RT. Thus, by increasing the transcriptional activity of IRF3/7 in cancer cells, this work could have important implications for the use of NBTXR3 activated by RT with immunotherapy.

Experimental

Cell line and culture conditions

The HCT116-DUAL cell line, derived from HCT116 human colorectal cancer cells, was purchased from InvivoGen. HCT116-DUAL cells contain the *Lucia luciferase* gene coding for the secreted form of the enzyme, under the control of an ISG54 minimal promoter in conjunction with five IFN-stimulated response elements,

* Corresponding author at: Nanobiotix, 60 rue de Wattignies, 75012 Paris, France.
E-mail address: sebastien.paris@nanobiotix.com (S. Paris).

https://doi.org/10.1016/j.radonc.2019.07.029
0167-8140/

recognized by the transcriptional factor IRF3/7. Cells were grown according to manufacturer's recommendations. Cells used in the experiments were controlled for mycoplasma. Using a clonogenic assay, we have previously reported that 800 μM was the most efficient tested concentration of NBTXR3 to kill HCT116 cancer cells, under RT [14]. This concentration was used for all presented experiments.

Radiotherapy

Cells were irradiated with 1 Gy to 4 Gy according to the study, delivered as a single dose, using the CellRad (Faxitron) operating at 150 kV.

Flow cytometry

Flow cytometry analyses were performed on Accuri C6+ (BD). Flow data were quantified using BD CSampler Plus software v.1.0.23.1 (BD).

Cell death analysis

Cell death analysis was performed using Annexin V-FITC kit (Miltenyi Biotec), according to manufacturer's instructions. Briefly, 2×10^5 cells were seeded in 6-well plates overnight. Then, media were replaced with 2 mL of fresh culture medium containing NBTXR3 or vehicle, overnight. Plates were then irradiated with 2 Gy or 4 Gy. Cell staining (Annexin V-FITC/PI) was performed at 48 h post-RT and analyzed by flow cytometry.

DNA double strand breaks analysis

DNA double strand breaks were analyzed by γ H2AX staining and flow cytometry. Briefly, 2.5×10^5 HCT116-DUAL cells were seeded in duplicate in 6-well plates. Cells were treated overnight with NBTXR3 or vehicle, then irradiated at 2 Gy or 4 Gy. Cells were harvested and fixed in ice cold EtOH 70% for 30 min after RT and incubated at −20 °C for 1 h. Then, cells were centrifuged, washed with PBS 1X, and permeabilized for 5 min with PBS 1X, 0.1% Triton. Cells were washed in PBS 1X and pellets were resuspended in 500 μL of 2% BSA in PBS. After 30 min incubation at room temperature under gentle agitation, cells were pelleted and resuspended with 100 μL of AF488 mouse anti-γ-H2AX (ser139) antibody (BD) or AF488 mouse IgG1 γ Isotype antibody control (BD), transferred to 96-well U bottom plates, and incubated for 1 h at room temperature in the dark under gentle rocking. Cells were washed with PBS 1X, then analyzed by flow cytometry.

Micronuclei evaluation

Micronuclei (MN) were stained using the MicroFlow In Vitro kit from Litron according to manufacturer's instructions. Briefly, HCT116-DUAL cells were seeded at the density of 2×10^4 cells per well in 24-well plates. The next day, cells were treated overnight with NBTXR3 or vehicle, then irradiated at 2 Gy or 4 Gy. After irradiation, supernatants were removed and replaced by fresh medium. Cells were analyzed for MN formation 96 h after RT. Plates were placed on ice for 20 min, then media were replaced with 300 μL of Nucleic Acid Dye A working solution per well and plates were exposed to a light source. After 30 min, this solution was replaced with 1 mL of cold 1X Buffer Solution. Then, the Buffer

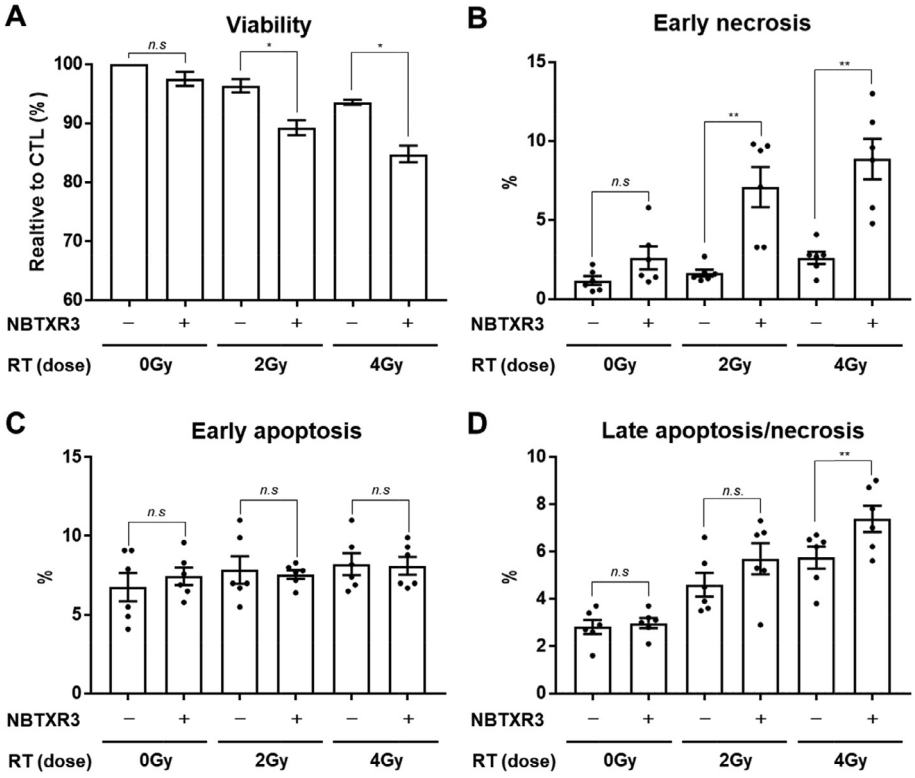

Fig. 1. NBTXR3 activated by RT results in more HCT116-DUAL cell death than RT alone. Percentages of (A) viability, (B) early necrosis, (C) early apoptosis and (D) late apoptosis/necrosis were assessed 48 h after RT by Annexin V-FITC/PI staining in HCT116-DUAL cell treated or not with 800 μM of NBTXR3 and irradiated with increasing doses of RT. Presented data were obtained from three independent experiments ($n = 3$) performed in duplicate (each dot represents one value). Data are represented as mean ± SEM. Statistical test: two-tailed *t*-test (C, D) or Mann–Whitney test (A, B). *n.s.*, not significant; *, $p < 0.05$;**, $p < 0.01$.

Solution was replaced with 500 µL of Complete Lysis Solution 1 and plates were gently mixed for 5 seconds on a vortex and incubated for one hour in the dark at 37 °C. Counting Beads (Life Technologies) were added and mixed with Complete Lysis Solution 2 then 500 µL of this mixture was added to each well. After 30 min incubation in the dark at room temperature, MN were analyzed by flow cytometry.

IRF activity assay

Luciferase activity, reflecting IRF3/7 transcriptional activity, was measured to evaluate cGAS-STING pathway activation in HCT116-DUAL cells after RT. Cells were seeded in 96-well plates at a density of 1×10^4 or 5×10^3 cells per well for 24 h or 96 h after RT analyses, respectively. The next day, cells were treated overnight with NBTXR3, in six-plicate, then irradiated (0, 1, 2, 3 or 4 Gy). After 24 h and 96 h, the supernatants were harvested, and Luciferase activity measured using the GloMax-96 Microplate luminometer (Promega) and the QUANTI-luc assay (InvivoGen), prepared according to manufacturer's recommendations. For Luciferase activity measurement, 20 µL of each supernatant were added into a well of a 96-well white plate, then placed into the luminometer.

Statistical analyses

The studies have been independently repeated at least three times. Results are expressed as mean ± SEM. For cGAS-STING pathway activation, measures were expressed as fold-increase relative to untreated cells. Normality distribution of values and homogeneity of variances were assessed by Shapiro–Wilk normality test and Brown–Forsythe test, respectively. Experiments with normal distribution and non-significant variances were analyzed by one-way ANOVA, Sidak's multiple comparison parametric test or by two-tailed *t*-test. Experiments with non-normal distribution and/or significant variances were analyzed by one-way ANOVA, Kruskal–Wallis and Dunn's correction for multiple comparison non-parametric test or Mann–Whitney test. A p value <0.05 was considered statistically significant. GraphPad Prism 7.04 software was used to perform statistical analyses.

Results and discussion

We first examined the ability of NBTXR3 activated by radiotherapy (NBTXR3+RT) to kill cancer cells, compared to RT alone. For this study, HCT116-DUAL cells were treated with NBTXR3, then irradiated with increasing doses. The different cellular physiological states (e.g. viability, early apoptosis, early necrosis and late apoptosis/necrosis) were measured 48 h after RT by Annexin V-FITC/propidium iodide staining and flow cytometry (Fig. 1) [16]. Analysis of cell viability indicated that addition of NBTXR3 (not activated by RT) has no effect, when compared to untreated cells. In contrast, NBTXR3+RT significantly decreased cell viability compared to RT alone (2 Gy, 96.3%±1.14 vs. 2 Gy+NBTXR3, 89.3%±1.24, $p < 0.05$, and 4 Gy, 93.5%±0.75 vs. 4 Gy+NBTXR3, 84.8%±2.48, $p < 0.05$). Interestingly, there results are in good accordance with our previously published results of clonogenic assay with HCT116 cells [14].

Cells treated with RT alone had a slight increase in markers of early necrosis, but nothing significant was observed. Conversely, NBTXR3+RT significantly increased early necrosis markers compared to RT alone (2 Gy, 1.6%±0.22 vs. 2 Gy+NBTXR3, 7.1% ± 1.27, $p < 0.01$, and 4 Gy, 2.6%±0.39 vs. 4 Gy+NBTXR3, 8.9% ± 1.28, $p < 0.01$). Furthermore, NBTXR3+RT increased late apoptosis/necrosis when compared to RT alone, but this difference was significant only at the highest dose tested (4 Gy, 5.7%±0.47 *vs.* 4 Gy+NBTXR3, 7.4%±1.36, $p < 0.01$). These results were in stark contrast to analysis of markers of early apoptosis, where no significant effect was observed across all conditions tested.

Since the main cytotoxic effect of RT is linked to its ability to generate DSBs, we next sought to determine if the significant increase of cell death triggered by NBTXR3+RT could be correlated to a larger production of DSBs. To verify this hypothesis, we assessed DSBs formation by γ H2AX foci staining and flow cytometry 30 min after RT (Fig. 2A). As expected, RT generated a significant dose-dependent increase of γ H2AX positive cell percentages at 2 Gy (7% ± 0.6, $p < 0.0001$), compared to untreated cells (0.9% ± 0.06). For NBTXR3+RT treated cells, the percentages of γ H2AX positive cells were significantly enhanced, compared to RT alone (7% ± 0.6 *vs.* 11.2% ± 0.38, $p < 0.001$, for 2 Gy *vs.* 2 Gy +NBTXR3; 16.9% ± 0.29 *vs.* 24.4% ± 1.07, $p < 0.0001$ for 4 Gy *vs.* 4 Gy+NBTXR3). This shows that DSBs formation was improved by RT activation of NBTXR3.

X-ray induced formation of micronuclei (MN) is generally thought to result from DNA double strand breaks [17,18], despite other mechanisms could occur [19]. In addition, MN have been

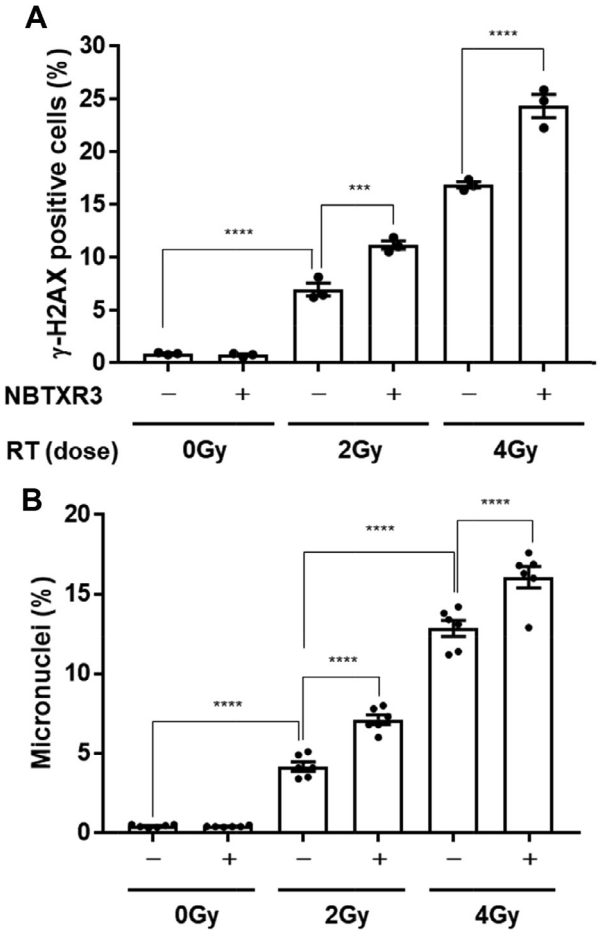

Fig. 2. NBTXR3 activated by RT enhances both DNA double strand breaks and micronuclei (MN) formation compared to RT alone. A, DNA double strand breaks analyses were assessed by γ H2AX staining 30 min after RT, in HCT116-DUAL treated or not with 800 µM of NBTXR3 and irradiated with increasing doses of RT. Data are means ± SEM, where each dot represents one independent experiment ($n = 3$). B, Micronuclei formation was assessed 96 h after RT, in HCT116-DUAL treated or not with 800 µM of NBTXR3 and irradiated with increasing doses of RT. Data are means ± SEM, where each dot represents one independent experiment ($n = 6$). Statistical test: one-way ANOVA, Sidak's multiple comparison parametric test. ***, $p < 0.001$; ****, $p < 0.0001$.

A

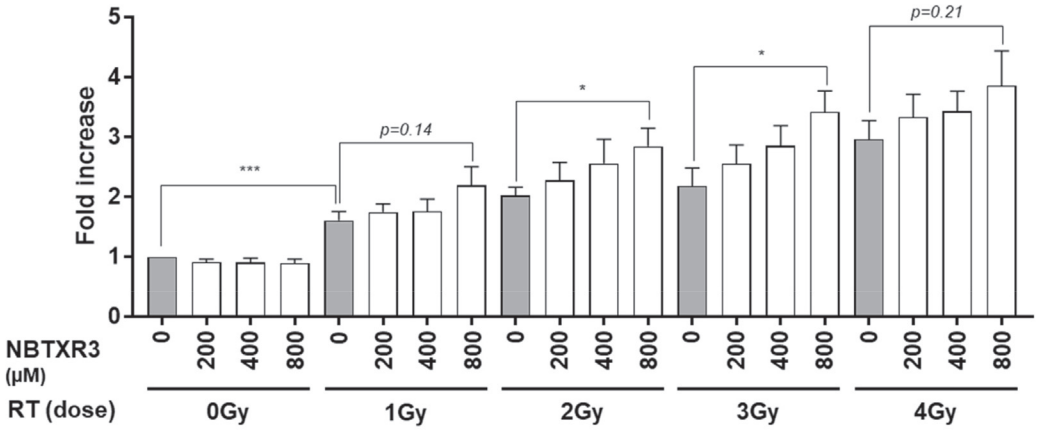

B

RT (Gy)	NBTXR3 (μM)	Mean increase (%) ± SEM	*p* value
1	200	8.8±2.09	0.52
	400	8.8±5.12	0.57
	800	34.7±8.93	0.14
2	200	11.1±7.58	0.45
	400	23.4±11.65	0.24
	800	39.8±6.39	0.04 (*)
3	200	18.4±8.05	0.42
	400	31.7±3.77	0.19
	800	60.3±16.32	0.04 (*)
4	200	12.5±4.91	0.47
	400	18.0±12.05	0.34
	800	29.0±8.40	0.21

Fig. 3. NBTXR3 activated by RT activates more efficiently cGAS-STING, compared to RT alone. A, cGAS-STING pathway activation was assessed by Luciferase activity measurement 96 h after RT, in HCT116-DUAL treated or not with growing doses of NBTXR3 and irradiated with increasing doses of RT. Data are represented as mean ± SEM of independent experiments ($n \geq 3$). Statistical test: two-tailed *t*-test. *, $p < 0.05$; ***, $p < 0.001$. B, Mean increase percentage of Luciferase activity after NBTXR3 activated by RT treatment, compared to RT alone.

clearly associated with activation of the cGAS-STING pathway [20–22]. We wanted to determine if the significant increase of DSBs measured in cells treated with NBTXR3+RT could in turn yield an increased amount of MN. To test this hypothesis, MN formation was evaluated by flow cytometry 96 h after RT (Fig. 2B). Both RT and NBTXR3+RT generated a significant dose-dependent increase of MN at all the tested doses ($p < 0.0001$), compared to untreated cells. However, the percentages of MN for cells treated with NBTXR3+RT were significantly higher, compared to RT alone (4.2% ± 0.29 *vs.* 7.1% ± 0.3, $p < 0.001$, for 2 Gy *vs.* 2 Gy+NBTXR3; 12.8% ± 0.51 *vs.* 16.1% ± 0.67, $p < 0.0001$ for 4 Gy *vs.* 4 Gy+NBTXR3), showing that NBTXR3+RT was more efficient than RT alone to induce MN formation.

Recent studies have demonstrated that RT increases genome-derived cytosolic DNA, mediating the activation of the cGAS-STING pathway [20–24]. Vanpouille-Box et al. reported in the mouse mammary adenocarcinoma TSA cells that transcription of IRF3 target genes could be detected as early as 24 h [24]. However, generation of micronuclei takes longer as cell must undergo mitosis following RT induced cell cycle arrest and DSB repair. Therefore, we wanted to assess if DSBs and/or MN produced after NBTXR3+RT treatment could trigger a higher activation of the cGAS-STING pathway. To explore this further, cells were irradiated with increasing doses of RT (1 to 4 Gy) with NBTXR3 and Luciferase activities were measured at 24 h and 96 h after RT.

After 24 ht, regardless of the condition, no significant variation in relative fold increase of Luciferase activity was observed (Fig. S1). This suggests that production of DSBs for irradiated conditions was not sufficient to generate a detectable activation of the cGAS-STING pathway in these cells. In contrast, after 96 h, a marked increase in relative fold increase Luciferase activity was observed, irrespective of the RT condition tested (Fig. 3). When compared to RT alone, relative Luciferase activities of cells irradiated with NBTXR3 were greatly increased, ranging from approximately 30 to 60% (Table 1). At 2 Gy and 3 Gy, the differences became significant ($p < 0.05$).

Conclusion

This article demonstrates that RT-activated NBTXR3 results in significantly more HCT116-DUAL cell death than RT alone, which is consistent with our previous *in vitro* and *in vivo* studies using wild-type HCT116 cells [13,14]. Thus, beyond the local control critical for patient survival, this implies that more immune-stimulating factors (i.e., Adenosine Triphosphate, Tumor-Associated Antigens) may be released by RT-activated NBTXR3

treatment compared to RT alone [25]. Interestingly, our results also show that, even at the highest dose tested (4 Gy), the biological effects of RT were inferior to those obtained for NBTXR3 at a lower dose of RT (2 Gy).

Induction of DNA double strand breaks by RT and subsequent formation of micronuclei are directly related to cGAS-STING activation [20–22,24]. NBTXR3 activated by RT generated significantly more DSBs and micronuclei than RT alone demonstrating the superior ability of this combination to damage DNA. Both elements were strong indicators for greater activation of the cGAS-STING pathway by NBTXR3 activated by RT, as demonstrated by the significant increase in Luciferase activity also measured in these cells. This increased activation of the cGAS-STING pathway may have effect on immune stimulation. Remarkably, our results also show a dose-dependency that suggests RT plus NBTXR3 can yield pathway activation equivalent to that obtained by a higher dose of RT alone (i.e., 1 Gy+NBTXR3 is equivalent to 3 Gy alone; 2 Gy+NBTXR3 is equivalent to 4 Gy alone). This striking result suggests that NBTXR3 could be used in situations where RT dose reduction is paramount to improve quality of life impacts from RT without changing the effectiveness of the RT-induced tumor cell death.

Taken together, these results demonstrate that RT-activated NBTXR3 could play an important role in the priming and/or enhancement of the antitumor immune response. To our knowledge, this is the first demonstration that nanoparticles with a physical mode of action were able to enhance cGAS-STING pathway activity of cancer cells via increased DNA damage, compared to RT alone. Taken together, these data support evaluating the rational combination of NBTXR3-enhanced RT and ICI, which should increase RT-mediated local tumor control and prime the immune system for greater systemic ICI response. This may have important implications for the use of irradiation in combination with immunotherapeutic agents. As such, a phase I/II trial was recently launched in patients with advanced cancers treated with NBXTR3, RT, and PD1 inhibitors (NCT03589339).

Declaration of Competing Interest

J. Marill, N. Mohamed Anesary and S. Paris are employees of Nanobiotix.

Acknowledgments

J. Marill, N. Mohamed Anesary and S. Paris are employees of Nanobiotix. The authors thank Dr. Katherine Jameson, Clinical Lead at Nanobiotix for proofreading this article and wise advice.

Appendix A. Supplementary data

Supplementary data to this article can be found online at https://doi.org/10.1016/j.radonc.2019.07.029.

References

[1] Harrington KJ, Billingham LJ, Brunner TB, Burnet NG, Chan CS, Hoskin P, et al. Guidelines for preclinical and early phase clinical assessment of novel radiosensitisers. Br J Cancer 2011;105:628–39.
[2] Liauw SL, Connell PP, Weichselbaum RR. New paradigms and future challenges in radiation oncology: an update of biological targets and technology. Sci Transl Med 2013;5:173sr2.
[3] Demaria S, Golden EB, Formenti SC. Role of local radiation therapy in cancer immunotherapy. JAMA Oncol 2015;1:1325–32.
[4] Sharabi AB, Lim M, DeWeese TL, Drake CG. Radiation and checkpoint blockade immunotherapy: radiosensitisation and potential mechanisms of synergy. Lancet Oncol 2015;16:e498–509.
[5] Apetoh L, Ghiringhelli F, Tesniere A, Obeid M, Ortiz C, Criollo A, et al. Toll-like receptor 4-dependent contribution of the immune system to anticancer chemotherapy and radiotherapy. Nat Med 2007;13:1050–9.
[6] Reits EA, Hodge JW, Herberts CA, Groothuis TA, Chakraborty M, Wansley EK, et al. Radiation modulates the peptide repertoire, enhances MHC class I expression, and induces successful antitumor immunotherapy. J Exp Med 2006;203:1259–71.
[7] Deng L, Liang H, Xu M, Yang X, Burnette B, Arina A, et al. STING-dependent cytosolic DNA sensing promotes radiation-induced type I interferon-dependent antitumor immunity in immunogenic tumors. Immunity 2014;41:843–52.
[8] Wang H, Hu S, Chen X, Shi H, Chen C, Sun L, et al. cGAS is essential for the antitumor effect of immune checkpoint blockade. Proc Natl Acad Sci U S A 2017;114:1637–42.
[9] Sharabi AB, Nirschl CJ, Kochel CM, Nirschl TR, Francica BJ, Velarde E, et al. Stereotactic radiation therapy augments antigen-specific PD-1-mediated antitumor immune responses via cross-presentation of tumor antigen. Cancer Immunol Res 2015;3:345–55.
[10] Wang L, Shureiqi I, Stroehlein JR, Wei D. Novel and emerging innate immune therapeutic targets for pancreatic cancer. Expert Opin Ther Targets 2018;22:977–81.
[11] Iurescia S, Fioretti D, Rinaldi M. Targeting cytosolic nucleic acid-sensing pathways for cancer immunotherapies. Front Immunol 2018;9:711.
[12] Levy L, Le Tourneau C, Sargos P, Le Pechoux C, Kantor G, de Baere T, et al. Hafnium oxide nanoparticles: an emergent promising treatment for solid tumors. CFS 2017. New-York2017.
[13] Maggiorella L, Barouch G, Devaux C, Pottier A, Deutsch E, Bourhis J, et al. Nanoscale radiotherapy with hafnium oxide nanoparticles. Future Oncol (London, England) 2012;8:1167–81.
[14] Marill J, Anesary NM, Zhang P, Vivet S, Borghi E, Levy L, et al. Hafnium oxide nanoparticles: toward an in vitro predictive biological effect? Radiation Oncol (London, England) 2014;9:150.
[15] Bonvalot S, Rutkowski PL, Thariat J, Carrère S, Ducassou A, Sunyach M-P, et al. NBTXR3, a frst-in-class radioenhancer hafnium oxide nanoparticle, plus radiotherapy versus radiotherapy alone in patients with locally advanced soft-tissue sarcoma (Act.In.Sarc): a multicentre, phase 2–3, randomised, controlled trial. Lancet Oncol 2019;20(8):1148–59.
[16] Wlodkowic D, Telford W, Skommer J, Darzynkiewicz Z. Apoptosis and beyond: cytometry in studies of programmed cell death. Methods Cell Biol 2011;103:55–98.
[17] Kashino G, Prise KM, Schettino G, Folkard M, Vojnovic B, Michael BD, et al. Evidence for induction of DNA double strand breaks in the bystander response to targeted soft X-rays in CHO cells. Mutat Res 2004;556:209–15.
[18] Kashino G, Suzuki K, Matsuda N, Kodama S, Ono K, Watanabe M, et al. Radiation induced bystander signals are independent of DNA damage and DNA repair capacity of the irradiated cells. Mutat Res 2007;619:134–8.
[19] Okada T, Kashino G, Nishiura H, Tano K, Watanabe M. Micronuclei formation induced by X-ray irradiation does not always result from DNA double-strand breaks. J Radiat Res 2012;53:93–100.
[20] Gekara NO. DNA damage-induced immune response: Micronuclei provide key platform. J Cell Biol 2017;216:2999–3001.
[21] Mackenzie KJ, Carroll P, Martin CA, Murina O, Fluteau A, Simpson DJ, et al. cGAS surveillance of micronuclei links genome instability to innate immunity. Nature 2017;548:461–5.
[22] Bartsch K, Knittler K, Borowski C, Rudnik S, Damme M, Aden K, et al. Absence of RNase H2 triggers generation of immunogenic micronuclei removed by autophagy. Hum Mol Genet 2017;26:3960–72.
[23] Erdal E, Haider S, Rehwinkel J, Harris AL, McHugh PJ. A prosurvival DNA damage-induced cytoplasmic interferon response is mediated by end resection factors and is limited by Trex1. Genes Dev 2017;31:353–69.
[24] Vanpouille-Box C, Alard A, Aryankalayil MJ, Sarfraz Y, Diamond JM, Schneider RJ, et al. DNA exonuclease Trex1 regulates radiotherapy-induced tumour immunogenicity. Nat Commun 2017;8:15618.
[25] Inoue H, Tani K. Multimodal immunogenic cancer cell death as a consequence of anticancer cytotoxic treatments. Cell Death Differ 2014;21:39–49.